



Cite This: J. Agric. Food Chem. 2018, 66, 856-865

pubs.acs.org/JAFC

# Comparison of Adaptive Neuroprotective Mechanisms of Sulforaphane and its Interconversion Product Erucin in in Vitro and in Vivo Models of Parkinson's Disease

Fabiana Morroni, †,‡ Giulia Sita, †,‡ Alice Djemil, Massimo D'Amico, Letizia Pruccoli, I Giorgio Cantelli-Forti, Patrizia Hrelia, and Andrea Tarozzi\*,

ABSTRACT: Several studies suggest that an increase of glutathione (GSH) through activation of the transcriptional nuclear factor (erythroid-derived 2)-like 2 (Nrf2) in the dopaminergic neurons may be a promising neuroprotective strategy in Parkinson's disease (PD). Among Nrf2 activators, isothiocyanate sulforaphane (SFN), derived from precursor glucosinolate present in Brassica vegetables, has gained attention as a potential neuroprotective compound. Bioavailability studies also suggest the contribution of SFN metabolites, including erucin (ERN), to the neuroprotective effects of SFN. Therefore, we compared the in vitro neuroprotective effects of SFN and ERN at the same dose level (5  $\mu$ M) and oxidative treatment with 6-hydroxydopamine (6-OHDA) in SH-SY5Y cells. The pretreatment of SH-SY5Y cells with SFN recorded a higher (p < 0.05) active nuclear Nrf2 protein (12.0  $\pm$  0.4 vs 8.0  $\pm$  0.2 fold increase), mRNA Nrf2 (2.0  $\pm$  0.3 vs 1.4  $\pm$  0.1 fold increase), total GSH (384.0  $\pm$  9.0 vs 256.0 ± 8.0 μM) levels, and resistance to neuronal apoptosis elicited by 6-OHDA compared to ERN. By contrast, the simultaneous treatment of SH-SY5Y cells with either SFN or ERN and 6-OHDA recorded similar neuroprotective effects with both the isothiocyanates (Nrf2 protein  $2.2 \pm 0.2$  vs  $2.1 \pm 0.1$  and mRNA Nrf2  $2.1 \pm 0.3$  vs  $1.9 \pm 0.2$  fold increase; total GSH  $384.0 \pm 4.8$  vs  $352.0 \pm 6.4 \mu M$ ). Finally, in vitro finding was confirmed in a 6-OHDA-PD mouse model. The metabolic oxidation of ERN to SFN could account for their similar neuroprotective effects in vivo, raising the possibility of using vegetables containing a precursor of ERN for systemic antioxidant benefits in a similar manner to SFN.

KEYWORDS: sulforaphane, erucin, 6-hydroxydopamine, Nrf2, Parkinson's disease

# ■ INTRODUCTION

A considerable amount of evidence supports a role for oxidative stress, mitochondrial dysfunction, and abnormal protein accumulation as early triggers of neuronal death in Parkinson's disease (PD) pathogenesis. 1,2 Glutathione (GSH) depletion is one of the earliest altered redox statuses in substantia nigra (SN) during the progression of PD, probably because of the presence of dopamine (DA) oxidative metabolism, iron, and a weak antioxidant and detoxifying defense system.<sup>3,4</sup>

Based on this evidence, it has been suggested that food-based approaches may be a promising strategy to prevent or slow the ongoing oxidative stress in PD. 5-7 Recent studies demonstrate the ability of dietary phytochemicals widely found in fruits and vegetables to reduce the neuronal death occurring in neurodegenerative diseases through several adaptive mechanisms. These mechanisms belong to the phenomenon called hormesis, including the activation of the nuclear factor (erythroid-derived 2)-like 2 (Nrf2), a master regulator of the antioxidant network and cytoprotective genes.<sup>8–10</sup> In this regard, emerging findings also suggest that hormesis involves the activation of multiple neuroprotective pathways that contribute to restore both mitochondrial dysfunction and abnormal protein accumulation in PD. 11,12 Among hormetic phytochemicals, the isothiocyanates (ITCs), derived from precursor glucosinolates, released from eating Brassica vegetables, have gained attention as

potential neuroprotective compounds with the ability to increase total GSH levels and related enzymes through the activation of Nrf2.<sup>13</sup> In particular, the electrophilic interaction of ITCs with the cysteine residues of the cytoplasmatic Kelchlike ECH-associated protein 1 (Keap1)-Nrf2 complex is a crucial event to promote the binding of Nrf2 with the antioxidant responsive element (ARE) at nuclear level.<sup>8</sup> Recent studies show multiple neuroprotective mechanisms of ITC sulforaphane (4-methyl-sulfinylbutyl ITC, SFN) in several in vitro and in vivo models of acute and chronic neurodegenerative disease. 14,15 The evidence of neuroprotective effects of SFN at central nervous system level must take into account the contribution of SFN tissue distribution and metabolites. SFN is released from precursor glucoraphanin, particularly abundant in watercress, broccoli, and broccoli sprouts, and, after the uptake in the organism, is conjugated with GSH and metabolized via the mercapturic acid pathway to its corresponding mercapturic acid derivate SFN-cysteinylglycine, SFN-cysteine, and SFN-Nacetylcysteine. 16 One interesting aspect is the reduction of the sulfoxide SFN to its thioether analogue erucin (4-methyl-

October 6, 2017 Received: Revised: December 29, 2017 Accepted: January 7, 2018 Published: January 7, 2018



<sup>&</sup>lt;sup>†</sup>Department of Pharmacy and Biotechnology, Alma Mater Studiorum—University of Bologna, Bologna, Italy

<sup>§</sup>Department of Experimental, Diagnostic and Specialised Medicine, General Pathology Unit, Alma Mater Studiorum—University of Bologna, Bologna, Italy

Department for Life Quality Studies, Alma Mater Studiorum—University of Bologna, Rimini, Italy

thiobutyl ITC, ERN), which is also metabolized via the mercapturic acid pathway and excreted in urine or bile. 16 ERN is also derived from glucoerucin, a major glucosinolate in Eruca sativa, and shows a similar biotransformation pathway and excretion fate to SFN (Figure 1). In particular, a biotransfor-

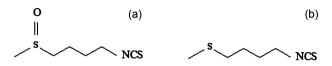


Figure 1. Chemical structure of (a) SFN and (b) ERN.

mation from ERN to SFN metabolites has been demonstrated. 16 In recent studies, ERN has shown a potential profile of antioxidant and neuroprotective effects similar to those observed with SFN. In particular, ERN increases hemeoxygenase (HO-1) expression and Nrf2 signaling in cultured human colon carcinoma HT29 cells and in mice, supporting our results that showed how a prolonged pretreatment of human dopaminergic neuroblastoma SH-SY5Y cells with ERN activated an antioxidant adaptive response against oxidative damage induced by 6-hydroxydopamine (6-OHDA). 17,18 Other studies suggest that biological effects elicited by ERN can be considered separately from those induced by SFN. 16 The determination of SFN and ERN in parallel is therefore a prerequisite for an adequate interpretation of their biological effects. 16

To compare the neuroprotective effects of ERN and SFN we determined their neuroprotective effects, in an in vitro and in vivo 6-OHDA-PD model, at the same dose level and treatment before or during the oxidant treatment with 6-OHDA. In particular, to mimic the neuronal transient oxidant events due to the DA in PD, we used an in vitro PD model characterized by a short oxidant treatment of SH-SY5Y cells with 6-OHDA and subsequent removal of the oxidant treatment to trigger the impairment of the neuronal redox status and neuronal death. This in vitro experimental approach allowed us to evaluate: (i) the time course of the SFN and ERN adaptive hormetic response in the absence of oxidant treatment as well as the ability of the adaptive hormetic response recorded with SFN and ERN to prevent the subsequent oxidative damage elicited by 6-OHDA; (ii) the neuroprotective adaptive response of SFN and ERN that occurs over time by successive short treatments with SFN or ERN and 6-OHDA.

# MATERIALS AND METHODS

Chemicals. ERN and SFN (both with purity ≥98%) were purchased from LKT Laboratories (LKT Laboratories, St. Paul, MN, USA); 6-OHDA, 2',7'-dichlorodihydrofluorescein diacetate (H<sub>2</sub>DCF-DA), anti- $\beta$ -actin and Nrf2 antibodies, apomorphine, and monochlorobimane were purchased from Sigma-Aldrich (Sigma-Aldrich, St. Louis, MO, USA). The anti-tyrosine hydroxylase (TH) antibody was purchased from Millipore (Millipore, Temecula, CA, USA). Annexin-V-FLUOS Staining Kit, Cell Death Detection ELISA PLUS kit, aprotinin, leupeptin, and NP-40 were purchased from Roche Diagnostics(Roche Diagnostics, Mannheim, Germany). RNA-tocDNA Kit, Taqman Universal Master Mix II, and Taqman probe for Nrf2 gene (ID: Hs00975961 g1) were purchased from Applied Biosystem Inc. (Applied Biosystem Inc., Foster City, CA, USA). The Nuclear Extract Kit and the TransAM Nrf2 Kit were purchased from Active Motif (Active Motif, Carlsbad, CA, USA). The goat biotinylated anti-rabbit IgG antibody and the DAB detection kit were purchased from Vector Laboratories (Burlingame, CA, USA). All reagents were of the highest grade of purity commercially available.

Cell Culture and Treatments. SH-SY5Y cell line was routinely grown at 37 °C in a humidified incubator with 5% CO<sub>2</sub> in Dulbecco's modified Eagle medium supplemented with 10% fetal bovine serum, 2 mM glutamine, 50 U/mL penicillin, and 50  $\mu$ g/mL streptomycin. To evaluate the neuronal redox status, SH-SY5Y cells were seeded in 96well plates at  $2 \times 10^4$  cells/well. To determine neuronal apoptosis parameters such as membrane phosphatidylserine exposure and DNA fragmentation into oligosomes, SH-SY5Y cells were seeded in culture dishes (size 100 mm) at  $1.5 \times 10^6$  cells/dish and in 96-well plates at  $2.5 \times 10^3$  cells/well, respectively. To evaluate active nuclear Nrf2 protein and total GSH levels, SH-SY5Y cells were seeded in culture dishes (size 60 mm) at  $2 \times 10^6$  cells/dish and in 96-well plates at  $2 \times$ 10<sup>4</sup> cells/well, respectively. All experiments were performed after 24 h of incubation at 37 °C in 5% CO<sub>2</sub>.

To evaluate the ability of SFN and ERN to modulate the neuronal basal levels of active nuclear Nrf2 protein, total GSH, and redox status without treatment with 6-OHDA, SH-SY5Y cells were treated with 5  $\mu$ M ITCs for 1, 3, 6, 12, and 24 h at 37 °C in 5% CO<sub>2</sub>. To determine the neuroprotective effects of SFN and ERN, SH-SY5Y cells were treated with 5  $\mu$ M ITCs 24 h before or during the treatment with 100  $\mu M$  6-OHDA for 2 h at 37 °C in 5% CO2. Next, the treatment was replaced with a medium without 6-OHDA and ITCs, and after further different incubation times we evaluated the nuclear active Nrf2 protein level (2 h), total GSH level (16 h), membrane phosphatidylserine exposure, and DNA fragmentation into oligosomes (16 h).

Quantitative Real-Time PCR on Nrf2 Gene Expression. RNA was extracted from SH-SY5Y cells using the RNeasy mini kit (Qiagen, Hilden, Germany) and following the manufacturer's procedures. cDNA was synthesized using the High capacity RNA-to-cDNA Kit. qRT-PCR was carried out using Taqman Universal Master Mix II, and the average mRNA fold change of Nrf2 gene was calculated by comparing the cycle threshold (Ct) of the target gene to that of the housekeeping gene 18-S rRNA. The Taqman probes span an exon junction. All reactions had three technical replicates, and each condition had three biological replicates. Relative quantification was calculated with the  $\Delta\Delta$ Ct method (2<sup>- $\Delta\Delta$ Ct</sup>).

Nuclear Extraction and Determination of Active Nrf2 Protein Level. Nuclear extraction and determination of active Nrf2 protein level were performed using the Nuclear Extract and TransAM Nrf2 Kit, respectively, according to the manufacturer's guidelines. The TransAM Nrf2 Kit is a DNA-binding ELISA able to determine the active Nrf2 protein level in nuclear extract. The primary antibody of the kit is able to recognize an epitope on Nrf2 protein upon ARE binding. The active Nrf2 protein levels in the treated cells are expressed as fold increase with respect to corresponding untreated cells.

Determination of Neuronal Redox Status. The neuronal redox status in terms of intracellular reactive oxygen species (ROS) levels was evaluated in SH-SY5Y cells as previously described with minor changes. 19 At the end of the treatment of SH-SY5Y cells, the culture medium was removed and 100  $\mu$ L of 2',7'-dichlorodihydrofluorescein diacetate,  $H_2DCF$ -DA (10  $\mu g/mL$ ), was added to each well. After 30 min of incubation at room temperature, the H2DCF-DA solution was replaced with phosphate buffer saline and the intracellular ROS levels were measured (excitation at 485 nm and emission at 535 nm) using a multilabel plate reader (VICTOR X3, PerkinElmer, Waltham, MA, USA). The values are expressed as arbitrary fluorescence units (AUF).

Determination of Membrane Phosphatidylserine Exposure. Apoptosis in terms of membrane phosphatidylserine exposure was evaluated using the Annexin-V-FLUOS Staining Kit, according to the manufacturer's instructions. The values are expressed as a percentage of annexin V positive cells.

Animals and Experimental Design. Male C57Bl/6 mice (9) weeks old, 25-30 g body weight; Harlan, Milan, Italy) were used for the experiments. All studies were performed in accordance with the Institutional Guidelines and complied with Italian regulations and associated guidelines of the European Communities Council Directive (PROT. n. 15-IX/9). The experimental protocol was based on the unilateral stereotaxic intrastriatal injection of 6-OHDA (AP, +0.5; ML, -2.0; DV, -2.5), as previously described. All animals tolerated the surgical operations well, and there was no mortality due to treatments. Animals were randomly divided into 4 groups (n=10-12 per group). Three groups received a 6-OHDA injection in the left striatum, while one group received the same volume of saline solution (sham group). One hour after brain lesion, we started intraperitoneal (ip) administration of either 30  $\mu$ mol/kg SFN or ERN or vehicle (VH, saline). We injected the mice twice a week. Thus, the four groups were sham/VH, 6-OHDA/VH, 6-OHDA/SFN, and 6-OHDA/ERN. Four weeks after the lesion, we assessed the extent of the lesion using the rotational behavior test. At the end of behavioral analysis, mice were sacrificed by cervical dislocation to perform neurochemical and immunohistochemical analysis.

The brains were removed and some of them were immersed in the fixative solution for 48 h, while in the others the SN was rapidly removed and placed into dry ice. SN samples were then homogenized in lysis buffer (50 mM Tris, pH 7.5, 0.4% NP-40, 10% glycerol, 150 mM NaCl, 10  $\mu$ g/mL aprotinin, 20  $\mu$ g/mL leupeptin, 10 mM EDTA, 1 mM sodium orthovanadate, 100 mM sodium fluoride), and protein concentration was determined by the Bradford method.

Rotational Behavior. All tests were carried out between 9.30 a.m. and 3.30 p.m. Animals were transferred to the experimental room at least 1 h before the test in order to let them acclimatize to the test environment. All scores were assigned by the same observer, who was unaware of the animal treatment. Apomorphine-induced rotations were determined 4 weeks after the surgical procedure, according to the method described earlier. Briefly, mice received a subcutaneous injection of apomorphine (0.05 mg/kg saline), a dopamine D1/D2 receptor agonist. They were acclimatized in plexiglass cylinders for 5 min prior to testing. After apomorphine administration, full body ipsilateral and contralateral turns were recorded using an overhead videocamera over a period of 10 min. Subsequently, each 360° rotation of the body axes was manually counted as a rotation. Values were expressed as the mean of contralateral turns collected during 10 min.

Western Blotting. As described,  $^{21}$  the protein lysates (30  $\mu g$  per sample) were separated by SDS-polyacrylamide gels and were transferred onto nitrocellulose membranes, which were probed with primary anti-TH and secondary antibodies. ECL reagents (Pierce, Rockford, IL, USA) were utilized to detect targeted bands. The same membranes were stripped and reprobed with  $\beta$ -actin antibody. Data were analyzed by densitometry, using Quantity One software (Bio-Rad). Values are expressed as fold increase versus respective contralateral intact site.

Immunohistochemistry. Fixed brains were sliced on a vibratome at 40 µm thickness. Sections were deparaffinized, hydrated through xylene, and rinsed in Tris-buffered saline (TBS). After deparaffinization, endogenous peroxidase was quenched with 3% H<sub>2</sub>O<sub>2</sub>. Nonspecific adsorption was minimized by incubating the section in 10% normal goat serum for 20 min. Sections were then incubated overnight, at 4 °C, with a rabbit anti-TH or anti-Nrf2 antibody, rinsed in TBS, and reincubated for 1 h, at room temperature, with a goat biotinylated anti-rabbit IgG antibody. Finally, sections were processed with the avidin-biotin technique, and reaction products were developed using commercial kits (Vector Laboratories). To verify the binding specificity, some sections were also incubated with only the primary antibody (no secondary) or with only the secondary antibody (no primary). In these situations, no positive staining was found in the sections, indicating that the immunoreactions were positive in all experiments carried out. Image analysis was performed by a blinded investigator, using an Axio Imager M1 microscope (Carl Zeiss, Oberkochen, Germany) and a computerized image analysis system (AxioCam MRc5, Zeiss) equipped with dedicated software (AxioVision Rel 4.8, Zeiss). After defining the boundary of the SN at low magnification (2.5× objective), the number of TH and Nrf2positive cells in the SN were counted on at least four adjacent sections at a higher magnification (10× objective). Positive cells were counted and compared to other experimental groups.

**Determination of DNA Fragmentation** *in Vitro* **and** *in Vivo*. The determination of DNA fragments into oligosomes was performed using the Cell Death Detection ELISA PLUS kit according to the manufacturer's guidelines. *In vitro* values are expressed as fold increase

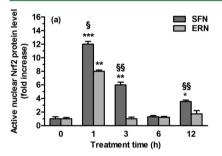
with respect to corresponding untreated cells. To determine the *in vivo* DNA fragmentation we used lysates corresponding to 80  $\mu$ g of protein, and the values are expressed as the mean of optical density fold increase with respect to the sham/VH group.

Determination of Total GSH Content in Vitro and in Vivo. Total GSH content in SH-SYSY cells was determined using the monochlorobimane assay in 96-well plates as previously reported. The values are expressed as concentrations of total GSH ( $\mu$ M) obtained by a GSH standard curve. Total GSH content in SN samples was estimated as described previously by us. The values are expressed as mmol of GSH/mg of total lysate proteins per assay.

**Statistical Analysis.** Data are reported as mean  $\pm$  SEM. Statistical analysis was performed using one-way ANOVA with Bonferroni post hoc test and Pearson's correlation coefficient for relations among variables. Differences were considered significant at p < 0.05. Analyses were performed using PRISM 5 software (GraphPad Software, La Jolla, CA, USA).

#### ■ RESULTS AND DISCUSSION

In Vitro Neuroprotective Effects of SFN and ERN. Initially, we evaluated the ability of SFN and ERN to activate early neuronal adaptive mechanisms modulating the active nuclear Nrf2 protein, mRNA Nrf2, total GSH levels, and redox status in terms of intracellular ROS levels without oxidative treatment with 6-OHDA in SH-SY5Y cells. As reported in Figure 2a, increasing the time of treatment of SH-SY5Y cells



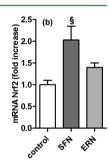


**Figure 2.** Effects of SFN and ERN on neuronal basal levels of active nuclear Nrf2 protein and mRNA Nrf2 in SH-SY5Y cells. (a) SH-SY5Y cells were treated for different lengths of time with 5 μM SFN or ERN in the absence of treatment with 6-OHDA. At the end of the treatment, active nuclear Nrf2 protein levels were measured as described in Materials and Methods. The nuclear Nrf2 protein values are expressed as fold increase with respect to untreated cells. Values are shown as mean ± SEM (n = 4-6). \*p < 0.05. \*\*p < 0.01 and \*\*\*\*p < 0.001 vs untreated cells; \*p < 0.05 and \*\*\*p < 0.01 vs cells treated with ERN; at ANOVA with Bonferroni post hoc test. (b) At the end of the 1 h treatment, Nrf2 mRNA relative expression was evaluated as described in Materials and Methods. The values were calculated through the  $2^{-\Delta\Delta Ct}$  method and expressed as fold increase with respect to untreated cells. Values are presented as mean ± SEM (n = 4-6). \*p < 0.05 vs cells treated with ERN; at ANOVA with Bonferroni post hoc test.

with either SFN or ERN 5  $\mu$ M, a concentration not associated with neurotoxicity (data not shown), showed that the highest increase of active nuclear Nrf2 protein levels occurred at 1 h. At this time, SFN recorded a significantly higher fold increase than ERN (12 vs 8). Less similar patterns of active nuclear Nrf2 protein levels were also determined at 3 and 12 h of treatment. The active nuclear Nrf2 protein levels recorded at 1 h were also accompanied by a similar compensation response of gene expression increase of mRNA Nrf2 as shown in Figure 2b. In parallel, comparable treatment times of SH-SY5Y cells with both the ITCs showed a significant decrease and increase of

total GSH and ROS levels, respectively (Figures 3a and 3b). Remarkably, SFN recorded significantly greater effects than

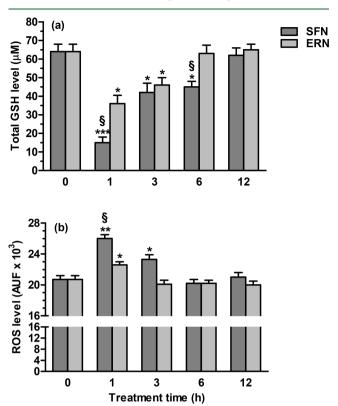


**Figure 3.** Effects of SFN and ERN on neuronal basal levels of total GSH and ROS in SH-SY5Y cells. (a, b) SH-SY5Y cells were treated for different lengths of time with 5  $\mu$ M SFN or ERN in the absence of treatment with 6-OHDA. At the end of the treatment, total GSH and ROS levels were measured as described in Materials and Methods. Total GSH values are expressed as concentrations of total GSH ( $\mu$ M) obtained by a GSH standard curve. The ROS values are expressed as arbitrary fluorescence units (AUF). Values are shown as mean  $\pm$  SEM (n = 4-6). \*p < 0.05, \*\*p < 0.01, and \*\*\*p < 0.001 vs untreated cells; \*p < 0.05 vs cells treated with ERN; at ANOVA with Bonferroni post hoc test.

ERN on total GSH basal levels at 1 h (percentage decrease, 77 vs 42) and 6 h (percentage decrease, 30 vs 2) as well as on ROS basal levels at 1 h (percentage increase, 30 vs 12) and 3 h (percentage increase, 15 vs 0). The highest magnitude of these effects recorded for both ITCs at 1 h decreased to basal levels when the treatment times of SH-SY5Y cells were extended to 12 h (Figures 3a and 3b).

As shown in Figures 4a and 4b, the higher activation of early adaptive mechanisms, specifically the increase of active nuclear Nrf2 protein and the total GSH depletion, induced by SFN compared to ERN was also prodromic in significantly different late adaptive mechanisms, such as increase and decrease in total neuronal GSH and ROS levels, respectively, at 24 h of treatment. At this treatment time, we recorded a significant inverse correlation between ROS and GSH levels for both SFN (r = -0.76, p < 0.01) and ERN (r = -0.93, p < 0.001) (Figure 4c). Subsequently, we evaluated the impact of different total GSH levels recorded after treatment with either SFN or ERN on prevention of neuronal apoptosis, in terms of membrane phosphatidylserine exposure (annexin V binding) and DNA fragmentation into oligosomes elicited by 6-OHDA in SH-

SY5Y cells. The pretreatment of SH-SY5Y cells for 24 h with either SFN or ERN 5  $\mu$ M led to a significant decrease of annexin V labeled cells induced by 2 h treatment with 6-OHDA and subsequent 16 h treatment without 6-OHDA (Figure 4d). The antiapoptotic effects of SFN were significantly higher than those of ERN, with a maximum inhibition of 95% and 60% respectively. These effects were confirmed by the higher ability of SFN to also reduce the DNA fragmentation into oligosomes induced by 6-OHDA than ERN at 5  $\mu$ M (Figure 4e). SFN and ERN alone did not change neuronal apoptosis basal levels (data not shown).

Taken together, these *in vitro* results show that the higher ability of SFN to prevent the neuronal death induced by 6-OHDA in SH-SY5Y cells compared to ERN could be ascribed to their different ability to activate upstream early adaptive mechanisms of GSH synthesis. In this regard, for the first time we demonstrated the greater ability of SFN to promote the nuclear Nrf2 activation as well as the increase of GSH than ERN in neuronal SH-SY5Y cells. Interestingly, these findings also suggest the determining contribution of GSH in maintaining redox balance and neuronal survival. Recent studies demonstrate that Nrf2 knockdown by siRNA in SH-SY5Y cells abolishes the intracellular GSH augmentation and the cellular protection elicited by SFN and other neuro-protective molecules.<sup>23–25</sup>

The different ability of SFN and ERN to activate a neuroprotective adaptive response through nuclear Nrf2 activation is consistent with the evidence that SFN containing oxidized sulfur is likely to be a more potent electrophilic ITC and phase II inducer than analogues containing nonoxidized sulfur, such as ERN. 26,27 Recent studies show that the electrophilic interaction of SFN with several cysteine residues in Keap1, particularly C151, inhibits the Keap1-dependent degradation of Nrf2 and increases the nuclear localization of Nrf2 as well as Nrf2 ARE-binding activity. 28,29 The higher electrophilicity of SFN than ERN also supports their different ability to induce a transient depletion of GSH through the intracellular conjugation of SFN and ERN with cellular nucleophiles including GSH, leading to increased levels of ROS. Other studies recorded similar transient pro-oxidant effects of SFN and ERN in non-neuronal cells, also suggesting a direct enzymatic redox regulation of GSH synthesis. In particular, the ROS formation with the depletion of GSH can lead to a conformational change in the catalytic subunit of gamma-glutamylcysteine synthetase, increasing its affinity for the substrates gamma-glutamic acid, cysteine, and adenosine triphosphate and thereby stimulating GSH synthesis.<sup>30</sup>

At present, we do not know the impact of the intracellular metabolism of SFN and ERN on their different abilities to activate neuronal adaptive mechanisms. In this regard, a recent study recorded the potential biotransformation of the same dose of SFN to the corresponding ERN metabolites at intracellular levels after 3 h of treatment. However, in view of the early nuclear Nrf2 activation elicited by both ITCs at 1 h as well as the lower ERN activity recorded we can presume that the intracellular reduction of SFN does not contribute to its highest activity.

In contrast to the experimental approach of pretreatment, the simultaneous treatment of SH-SY5Y with either SFN or ERN (5  $\mu$ M) and 6-OHDA (100  $\mu$ M) recorded similar neuroprotective effects with both the ITCs (Figure 5). Interestingly, both SFN and ERN significantly strengthened the increase of active nuclear Nrf2 protein and total GSH levels elicited by 6-

Journal of Agricultural and Food Chemistry

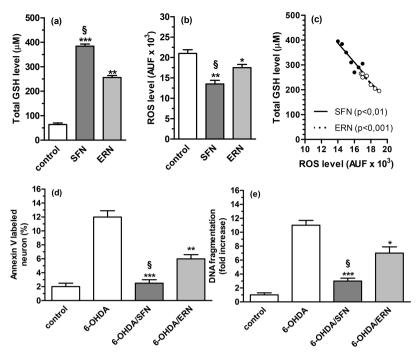


**Figure 4.** SFN and ERN improve neuronal redox status and prevent neuronal apoptosis induced by 6-OHDA in SH-SY5Y cells. (a, b) SH-SY5Y cells were treated for 24 h with 5 μM SFN or ERN in the absence of treatment with 6-OHDA. At the end of treatment, total GSH and ROS levels were measured as described in Materials and Methods. Total GSH values are expressed as concentrations of total GSH (μM) obtained by a GSH standard curve. ROS values are expressed as arbitrary fluorescence units (AUF). Values are shown as mean ± SEM (n = 4-6). \*p < 0.05 and \*\*p < 0.01 vs untreated cells; \*p < 0.05 vs cells treated with ERN; at ANOVA with Bonferroni post hoc test. (c) Correlation between total GSH and ROS levels recorded after 24 h of treatment with 5 μM SFN or ERN. (d, e) SH-SY5Y cells were treated for 24 h with 5 μM SFN or ERN and then with 6-OHDA (100 μM) for 2 h. Next, the treatment was replaced with a medium without 6-OHDA and ITCs, and after a further 16 h incubation we determined the neuronal apoptosis, in terms of membrane phosphatidylserine exposure (annexin V binding) and DNA fragmentation into oligosomes, as described in Materials and Methods. Values are expressed as percentage of annexin V labeled neurons and fold increase of DNA fragmentation with respect to untreated cells. Values are shown as mean ± SEM (n = 4-6). \*p < 0.05, \*\*p < 0.01, and \*\*\*p < 0.001 vs cells treated with 6-OHDA; \*p < 0.05 vs cells treated with 6-OHDA/ERN; \*p < 0.001 vs untreated cells; at ANOVA with Bonferroni post hoc test.

OHDA in SH-SY5Y cells at 2 and 16 h, respectively, after cotreatment with 6-OHDA (Figures 5a and 5c). The Nrf2-ARE binding activation was also matched by a similar profile of compensatory response of mRNA Nrf2 gene expression as shown in Figure 5b. In similar cotreatment conditions, both the ITCs also showed the ability to counteract the annexin V labeled cells and the DNA fragmentation into oligosomes at 16 h (Figures 6a and 6b).

This experimental approach highlights an adaptive stress response of the antioxidant network, specifically the GSH system, to oxidative damage of 6-OHDA. When the oxidative damage is too drastic, these adaptive systems fail, leading to neuronal death.<sup>30</sup> In this context, the neuroprotective effects of both ITCs could be ascribed to their ability to strengthen the GSH adaptive response at transcriptional level, ensuring neuronal survival. Interestingly, cotreatment with ERN and 6-OHDA recorded a neuroprotective effect similar to that of SFN, suggesting an *in vitro* interconversion of ERN in SFN favored by the oxidative reaction of 6-OHDA.

In Vivo Neuroprotective Effects of SFN and ERN. Four weeks after the lesion, we compared the neuroprotective effects of SFN and ERN against the oxidative damage induced by 6-OHDA in vivo. In particular, we evaluated the toxicity in dopaminergic neurons of mice after intrastriatal injection of 6-OHDA and ip administration of either 30  $\mu$ mol/kg SFN or ERN. First, we performed a behavioral quantification of dopamine depletion, by apomorphine-induced rotations 4 weeks after the induced lesion. As reported in Figure 7, the

intrastriatal injection of 6-OHDA significantly increased the number of apomorphine-induced rotations in lesioned mice compared with sham mice (p < 0.001, sham/VH vs 6-OHDA/ VH). Our results demonstrate that SFN and ERN induced a partial recovery in the rotational behavior test; in fact we still found a difference between the treatment groups and the sham operated mice. However, statistical analysis of the total net number of rotations showed that both SFN and ERN treatments counteracted the asymmetric motor behavior compared to the 6-OHDA/VH group (Figure 7, p < 0.05). These results were confirmed, as reported in Figure 8a, by the TH levels, a marker for dopaminergic neuronal function, which were significantly decreased in the SN of 6-OHDA-lesioned mice (85% vs sham/VH), and both SFN and ERN treatments strongly upregulated the expression of TH (78% and 74% respectively compared to the 6-OHDA/VH group, Figure 8a). To confirm this result, we also performed an immunohistochemical analysis on brain coronal slices containing SN structure (Figure 8b,c), and our results showed a consistent loss in dopaminergic neuronal function (93% vs sham/VH), efficiently counteracted by our treatments. Similarly, both SFN and ERN treatments protected neuronal tissue from apoptosis by significantly reducing DNA fragmentation in SN samples induced by intrastriatal injection of 6-OHDA (respectively 54% and 48% compared to the 6-OHDA/VH, Figure 8d). With regard to the neuroprotective effects of the ITCs, we did not find any significant differences between them (Figure 8).

Journal of Agricultural and Food Chemistry

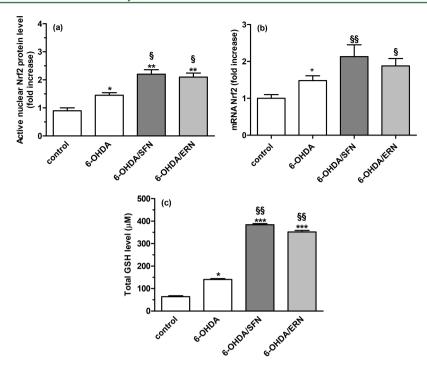


Figure 5. SFN and ERN strengthen Nrf2 and total GSH adaptive stress response elicited by 6-OHDA. (a, b) SH-SY5Y cells were treated with 6-OHDA (100  $\mu$ M) and either SFN or ERN (5  $\mu$ M) for 2 h. Next, the treatment was replaced with a medium without 6-OHDA and ITCs, and after a further 2 h incubation we determined the active nuclear Nrf2 protein levels and Nrf2 mRNA relative expression as described in Materials and Methods. Values are expressed as fold increase with respect to untreated cells. Values are shown as mean  $\pm$  SEM (n = 4). \*p < 0.05 and \*\*p < 0.01 vs untreated cells; \*p < 0.05 and \*\*p < 0.01 vs cells treated with 6-OHDA; at ANOVA with Bonferroni post hoc test. (c) SH-SY5Y cells were treated with 6-OHDA (100  $\mu$ M) and either SFN or ERN (5  $\mu$ M) for 2 h. Next, the treatment was replaced with a medium without 6-OHDA and ITCs, and after a further 16 h incubation we determined the total GSH levels as described in Materials and Methods. Values are expressed as fold increase with respect to untreated cells. Values are shown as mean  $\pm$  SEM (n = 4). \*p < 0.05 and \*\*\*p < 0.001 vs untreated cells; \*p < 0.01 vs cells treated with 6-OHDA; at ANOVA with Bonferroni post hoc test.

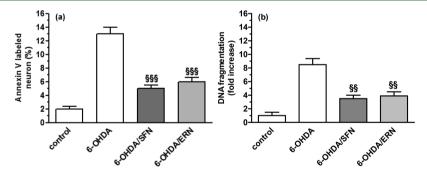


Figure 6. SFN and ERN counteract neuronal apoptosis induced by 6-OHDA in SH-SY5Y cells. (a, b) SH-SY5Y cells were treated with 6-OHDA (100  $\mu$ M) and either SFN or ERN (5  $\mu$ M) for 2 h. Next, the treatment was replaced with a medium without 6-OHDA and ITCs, and after a further 16 h incubation we determined the neuronal apoptosis, in terms of membrane phosphatidylserine exposure (annexin V binding) and DNA fragmentation into oligosomes, as described in Materials and Methods. Values are expressed as a percentage of annexin V labeled neurons and fold increase of DNA fragmentation with respect untreated cells. Values are shown as mean  $\pm$  SEM (n = 4). §§ p < 0.001 and §§§ p < 0.001 vs cells treated with 6-OHDA; at ANOVA with Bonferroni post hoc test.

As expected, when we measured GSH content it was significantly decreased (Figure 9a) in the 6-OHDA/VH group as compared to the sham/VH group. More interestingly, SFN and ERN consistently protected against the 6-OHDA-associated oxidative stress by maintaining GSH close to baseline values (Figure 9a). Remarkably, we did not record any differences between SFN and ERN in their ability to restore the GSH levels.

Previous studies in mice have shown the ability of SFN to increase the Nrf2 protein levels in various brain regions, including basal ganglia, leading to upregulation of phase II antioxidant enzymes in different stress conditions.<sup>31–34</sup> Among

the upregulation of antioxidant molecules and enzymes by Nrf2, we demonstrated the contribution of the increased GSH levels in striatum to the neuroprotective effects of SFN found in the 6-OHDA-PD mouse model.<sup>20</sup>

To confirm that the neuroprotective effects of SFN and ERN recorded against 6-OHDA are the consequence of the same upstream redox adaptive mechanisms, we also performed an immunostaining for Nrf2-positive cells on brain coronal slices containing SN structure (Figure 9b,c). As we expected, 4 weeks after the lesion was induced it was possible to observe a consistent loss in Nrf2 activity (45% vs sham/VH group), efficiently restored by the treatment with SFN or ERN, but we

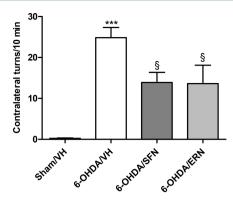


Figure 7. SFN and ERN ameliorate the performance on apomorphine-induced rotational behavior in 6-OHDA-lesioned mice. C57Bl/6 mice were treated ip (30  $\mu$ mol/kg) with either SFN or ERN twice a week for 4 weeks after intrastriatal injection of 6-OHDA. The number of net ipsi and contralateral rotations was counted for 10 min. Values are expressed as mean  $\pm$  SEM (n=10) of contralateral turns collected during 10 min. \*\*\*p < 0.001 vs sham/VH, p < 0.05 vs 6-OHDA/VH; at ANOVA with Bonferroni post hoc test.

did not find any difference between these ITCs in the inductive response. Interestingly, in the oxidative stress conditions the restoration of Nrf2 induced by both ITCs significantly exceeded basal levels of the sham/VH group, also suggesting the activation of long-term adaptive effects. It is plausible that, in addition to direct short-term adaptive effects on the GSH system elicited by 6-OHDA oxidative stress, the ITC treatment for 4 weeks strengthened the long-term adaptive effects in SN at transcriptional, epigenetic, and genomic level.<sup>30</sup>

Taken together, these results demonstrate for the first time that, in the presence of ongoing oxidative damage processes, ERN can exert similar *in vivo* neuroprotective effects to SFN. These findings are also supported by our *in vitro* results that recorded higher neuroprotective effects of SFN than ERN when we treated the neuronal cells with both ITCs before, but not during, the oxidative stress induced by 6-OHDA. Therefore, we can presume that the oxidation state of the sulfur in the side chain of ERN affects its ability to activate early prodromal adaptive mechanisms of neuroprotective effects.

Systemic metabolism may also play an important part in determining the neuroprotective activity of ERN *in vivo*. Several studies of bioavailability and biotransformation show that the

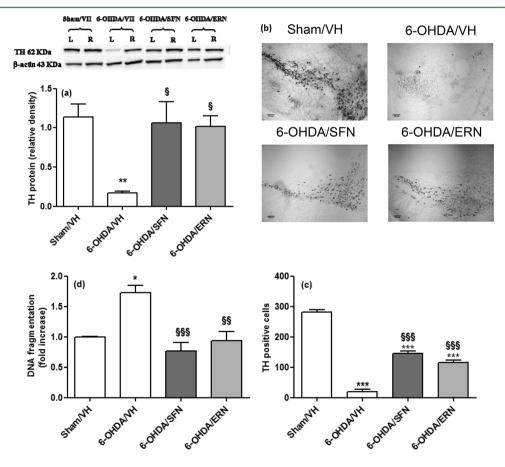


Figure 8. SFN and ERN counteract neuronal death and DNA fragmentation in 6-OHDA lesioned mice. (a, c) After 4 weeks of treatment with ITCs (30  $\mu$ mol/kg), TH protein levels were detected by (a) Western blotting and (b, c) immunohistochemistry in brain coronal sections containing SN. (a) Top: representative images of protein expression. Bottom: quantitative analysis of the Western blotting results for the TH protein levels in SN samples. Values were normalized to  $\beta$ -actin and expressed as mean of fold increase  $\pm$  SEM (n = 10) of each group compared to the intact control site. (b) Representative photomicrographs of immunostaining on lesioned side, scale bar 100  $\mu$ m. (c) Histogram representing dopaminergic cell survival in the SN. Values are expressed as mean  $\pm$  SEM (n = 10) of the percentage of surviving TH-positive cells of the lesioned hemisphere compared to the intact hemisphere. \*\*\*p < 0.001 vs sham/VH; §§§p < 0.01 vs 6-OHDA/VH; at ANOVA Bonferroni post hoc test. (d) DNA fragmentation was determined in SN samples as described in Materials and Methods. Values are expressed as mean of fold increase  $\pm$  SEM (n = 10). \*p < 0.05 vs sham/VH; §§p < 0.01 and §§§p < 0.001 vs 6-OHDA/VH; at ANOVA with Bonferroni post hoc test.

Journal of Agricultural and Food Chemistry

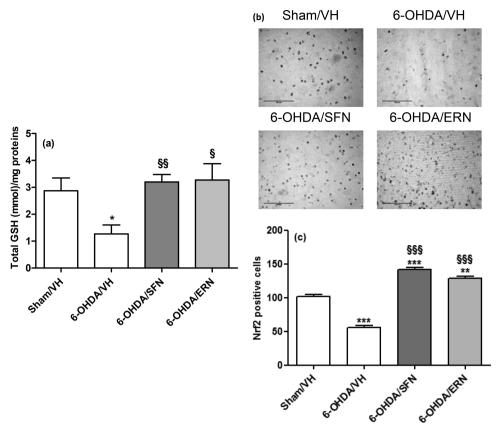


Figure 9. SFN and ERN increase total GSH and Nrf2 levels in 6-OHDA lesioned mice. After 4 weeks of treatment with ITCs (30  $\mu$ mol/kg), (a) total GSH and (b, c) Nrf2 levels were measured in SN samples as described in Materials and Methods. (a) Total GSH values are expressed as the mean of total GSH (mmol)/mg protein obtained by a GSH standard curve. Values are shown as mean  $\pm$  SEM (n = 10). (b) Representative photomicrographs of immunostaining for Nrf2 in brain coronal sections containing the SN, scale bar 100  $\mu$ m. (c) Quantitative analysis of the number of positive cells to Nrf2 activation. Values are expressed as mean  $\pm$  SEM (n = 10) of positive cells in each experimental group. \*p < 0.05, \*\*p < 0.01, and \*\*\*p < 0.001 vs sham/VH; \*p < 0.05, \*\*p < 0.01, and \*\*\*p < 0.001 vs 6-OHDA/VH; at ANOVA with Bonferroni post hoc test.

sulfur of ERN is extensively oxidized in mice, rats, and humans, forming SFN, while SFN is partly reduced to ERN.35-37 In particular, the systemic metabolic interconversion of these ITCs would also account for their similar inductive antioxidant action in vivo (phase II enzyme activities). 26,38–40 However, this interpretation is speculative considering the limitation of our study, such as the lack of determination of SFN and ERN levels in mouse biological fluids. Although various studies recorded the ITC interconversion in similar mouse animal species, the contribution of this metabolic interconversion from ERN to SFN at brain level remains to be clarified. 16,35,40 A recent study in mice in the absence of oxidative stress conditions reported the ability of glucoerucin, a glucosinolate precursor of ERN, to induce the expression of the HO-1 gene upregulated by Nrf2 in the intestinal mucosae and liver but not in the brain, reinforcing the hypothesis that the oxidative stress could play a more important role than the neuronal metabolism for the oxidation of ERN to SFN at brain level.18

Regarding the neuroprotective mechanisms of SFN and ERN, the *in vitro* experimental approach also allowed us to define the neuroprotective time window of dietary ITCs on PD initiation and progression. The higher neuroprotective effects of SFN than ERN recorded with a long treatment of neurons before the oxidative damage suggest that a chronic exposure to dietary SFN could reduce the risk of developing PD in healthy subjects. Instead, the similar neuroprotective effects obtained after a short combined treatment with SFN or ERN and 6-

OHDA indicate the potential ability of both dietary SFN and ERN to slow the neuronal transient oxidant events due to the DA in subjects with ongoing PD. In this regard, the effective relationship between the 5  $\mu M$  concentration of SFN and ERN used in our in vitro experiments and that occurring in humans is a concern. By contrast with other individual phytochemicals, the effective concentrations of ITCs in vitro are more likely to occur in vivo. 10 Our in vitro concentration level is routinely used in neuroprotection studies with SFN and very similar to the 2.2 and 7.4 µM concentrations of SFN in the human plasma after consumption of standard broccoli and high-glucosinolate broccoli, respectively. 41 In this regard, a more recent study in mouse model also detected comparable concentrations of total ITC metabolites in plasma  $(1-2 \mu M)$  as well as the conversion of ERN to SFN metabolites after isothiocyanate ERN oral gavage. 40 Overall, our findings and considerations support the development of vegetable products containing precursors of SFN and/or ERN for nutritional interventions aimed at preventing or delaying the progression of PD.

# AUTHOR INFORMATION

# **Corresponding Author**

\*Department for Life Quality Studies, Alma Mater Studiorum—University of Bologna, Corso D'Augusto 237, 47921 Rimini, Italy. Phone: +39 0541434620. Fax: +39 0541434607. E-mail: andrea.tarozzi@unibo.it.

#### ORCID ®

Andrea Tarozzi: 0000-0001-7983-8575

#### **Author Contributions**

<sup>‡</sup>F.M. and G.S. contributed equally to this work.

#### **Funding**

This work was supported by PRIN 2015 (Project 20152HKF3Z; Project 2015SKN9YT003).

### **Notes**

The authors declare no competing financial interest.

#### ACKNOWLEDGMENTS

We thank Susan West for the linguistic revision of the manuscript.

# ABBREVIATIONS USED

6-OHDA, 6-hydroxydopamine; ARE, antioxidant responsive element; AUF, arbitrary fluorescence units; ERN, 4-methylthiobutyl isothiocyanate (Erucin); DA, dopamine; GSH, glutathione; HO-1, heme oxygenase 1; H<sub>2</sub>DCF-DA, 2′,7′-dichlorodihydrofluorescein diacetate; H<sub>2</sub>O<sub>2</sub>, hydrogen peroxide; Keap-1, Kelch-like ECH-associated protein 1; ip, intraperitoneal; ITCs, isothiocyanates; Nrf2, nuclear factor (erythroid-derived 2)-like 2; PD, Parkinson's disease; ROS, reactive oxygen species; SFN, 4-methyl-sulfinylbutyl isothiocyanate (sulforaphane); SN, substantia nigra; TH, tyrosine Hydroxylase; TBS, Tris-buffered saline; VH, vehicle

# REFERENCES

- (1) Jenner, P.; Olanow, C. W. The pathogenesis of cell death in Parkinson's disease. *Neurology* **2006**, *66* (10, Suppl. 4), S24–S36.
- (2) Blesa, J.; Trigo-Damas, I.; Quiroga-Varela, A.; Jackson-Lewis, V. R. Oxidative stress and Parkinson's disease. *Front. Neuroanat.* **2015**, *9*, 91.
- (3) Dias, V.; Junn, E.; Mouradian, M. M. The role of oxidative stress in Parkinson's disease. *J. Parkinson's Dis.* **2013**, 3 (4), 461–491.
- (4) Mazzetti, A. P.; Fiorile, M. C.; Primavera, A.; Lo Bello, M. Glutathione transferases and neurodegenerative diseases. *Neurochem. Int.* **2015**, 82, 10–18.
- (5) Athauda, D.; Foltynie, T. The ongoing pursuit of neuroprotective therapies in Parkinson disease. *Nat. Rev. Neurol.* **2015**, *11* (1), 25–40.
- (6) Hang, L.; Basil, A. H.; Lim, K.-L. Nutraceuticals in Parkinson's Disease. *NeuroMol. Med.* **2016**, *18* (3), 306–321.
- (7) Dadhania, V. P.; Trivedi, P. P.; Vikram, A.; Tripathi, D. N. Nutraceuticals against Neurodegeneration: A Mechanistic Insight. *Curr. Neuropharmacol.* **2016**, *14* (6), 627–640.
- (8) Zhang, M.; An, C.; Gao, Y.; Leak, R. K.; Chen, J.; Zhang, F. Emerging roles of Nrf2 and phase II antioxidant enzymes in neuroprotection. *Prog. Neurobiol.* **2013**, *100*, 30–47.
- (9) Calabrese, V.; Cornelius, C.; Dinkova-Kostova, A. T.; Calabrese, E. J.; Mattson, M. P. Cellular stress responses, the hormesis paradigm, and vitagenes: novel targets for therapeutic intervention in neuro-degenerative disorders. *Antioxid. Redox Signaling* **2010**, *13* (11), 1763–1811
- (10) Qin, S.; Hou, D.-X. Multiple regulations of Keap1/Nrf2 system by dietary phytochemicals. *Mol. Nutr. Food Res.* **2016**, *60* (8), 1731–1755.
- (11) Mollereau, B.; Rzechorzek, N. M.; Roussel, B. D.; Sedru, M.; Van den Brink, D. M.; Bailly-Maitre, B.; Palladino, F.; Medinas, D. B.; Domingos, P. M.; Hunot, S.; et al. Adaptive preconditioning in neurological diseases therapeutic insights from proteostatic perturbations. *Brain Res.* **2016**, *1648* (Part B), 603–616.
- (12) Raefsky, S. M.; Mattson, M. P. Adaptive responses of neuronal mitochondria to bioenergetic challenges: Roles in neuroplasticity and disease resistance. *Free Radical Biol. Med.* **2017**, *102*, 203–216.

- (13) Giacoppo, S.; Galuppo, M.; Montaut, S.; Iori, R.; Rollin, P.; Bramanti, P.; Mazzon, E. An overview on neuroprotective effects of isothiocyanates for the treatment of neurodegenerative diseases. *Fitoterapia* **2015**, *106*, 12–21.
- (14) Tarozzi, A.; Angeloni, C.; Malaguti, M.; Morroni, F.; Hrelia, S.; Hrelia, P. Sulforaphane as a potential protective phytochemical against neurodegenerative diseases. *Oxid. Med. Cell. Longevity* **2013**, *2013*, 415078.
- (15) Sita, G.; Hrelia, P.; Tarozzi, A.; Morroni, F. Isothiocyanates are promising compounds against oxidative stress, neuroinflammation and cell death that may benefit neurodegeneration in Parkinson's disease. *Int. J. Mol. Sci.* **2016**, *17* (9), 1454.
- (16) Platz, S.; Piberger, A. L.; Budnowski, J.; Herz, C.; Schreiner, M.; Blaut, M.; Hartwig, A.; Lamy, E.; Hanske, L.; Rohn, S. Bioavailability and biotransformation of sulforaphane and erucin metabolites in different biological matrices determined by LC-MS-MS. *Anal. Bioanal. Chem.* **2015**, 407 (7), 1819–1829.
- (17) Tarozzi, A.; Morroni, F.; Bolondi, C.; Sita, G.; Hrelia, P.; Djemil, A.; Cantelli-Forti, G. Neuroprotective effects of erucin against 6-hydroxydopamine-induced oxidative damage in a dopaminergic-like neuroblastoma cell line. *Int. J. Mol. Sci.* **2012**, *13* (9), 10899–10910.
- (18) Wagner, A.; Sturm, C.; Piegholdt, S.; Wolf, I.; Esatbeyoglu, T.; De Nicola, G.; Iori, R.; Rimbach, G. Myrosinase-treated glucoerucin is a potent inducer of the Nrf2 target gene heme oxygenase 1–studies in cultured HT-29 cells and mice. *J. Nutr. Biochem.* **2015**, 26 (6), 661–666
- (19) Tarozzi, A.; Morroni, F.; Merlicco, A.; Hrelia, S.; Angeloni, C.; Cantelli-Forti, G.; Hrelia, P. Sulforaphane as an inducer of glutathione prevents oxidative stress-induced cell death in a dopaminergic-like neuroblastoma cell line. *J. Neurochem.* **2009**, *111* (5), 1161–1171.
- (20) Morroni, F.; Tarozzi, A.; Sita, G.; Bolondi, C.; Zolezzi Moraga, J. M.; Cantelli-Forti, G.; Hrelia, P. Neuroprotective effect of sulforaphane in 6-hydroxydopamine-lesioned mouse model of Parkinson's disease. *NeuroToxicology* **2013**, *36*, 63–71.
- (21) Morroni, F.; Sita, G.; Tarozzi, A.; Cantelli-Forti, G.; Hrelia, P. Neuroprotection by 6-(methylsulfinyl)hexyl isothiocyanate in a 6-hydroxydopamine mouse model of Parkinson's disease. *Brain Res.* **2014**, *1589*, 93–104.
- (22) Sebastià, J.; Cristòfol, R.; Martín, M.; Rodríguez-Farré, E.; Sanfeliu, C. Evaluation of fluorescent dyes for measuring intracellular glutathione content in primary cultures of human neurons and neuroblastoma SH-SYSY. *Cytometry, Part A* **2003**, *51A* (1), 16–25.
- (23) de Oliveira, M. R.; de Bittencourt Brasil, F.; Fürstenau, C. R. Sulforaphane Promotes Mitochondrial Protection in SH-SY5Y Cells Exposed to Hydrogen Peroxide by an Nrf2-Dependent Mechanism. *Mol. Neurobiol.* **2017**, DOI: 10.1007/s12035-017-0684-2.
- (24) de Oliveira, M. R.; Brasil, F. B.; Andrade, C. M. B. Naringenin Attenuates H2O2-Induced Mitochondrial Dysfunction by an Nrf2-Dependent Mechanism in SH-SY5Y Cells. *Neurochem. Res.* **2017**, 42 (11), 3341–3350.
- (25) Zhang, N.; Shu, H.-Y.; Huang, T.; Zhang, Q.-L.; Li, D.; Zhang, G.-Q.; Peng, X.-Y.; Liu, C.-F.; Luo, W.-F.; Hu, L.-F. Nrf2 Signaling Contributes to the Neuroprotective Effects of Urate against 6-OHDA Toxicity. *PLoS One* **2014**, *9* (6), e100286.
- (26) Zhang, Y.; Talalay, P.; Cho, C. G.; Posner, G. H. A major inducer of anticarcinogenic protective enzymes from broccoli: isolation and elucidation of structure. *Proc. Natl. Acad. Sci. U. S. A.* **1992**, 89 (6), 2399–2403.
- (27) Fahey, J. W.; Talalay, P. Antioxidant functions of sulforaphane: a potent inducer of Phase II detoxication enzymes. *Food Chem. Toxicol.* **1999**, *37* (9–10), 973–979.
- (28) Zhang, D. D.; Hannink, M. Distinct cysteine residues in Keap1 are required for Keap1-dependent ubiquitination of Nrf2 and for stabilization of Nrf2 by chemopreventive agents and oxidative stress. *Mol. Cell. Biol.* **2003**, 23 (22), 8137–8151.
- (29) Hu, C.; Eggler, A. L.; Mesecar, A. D.; van Breemen, R. B. Modification of keap1 cysteine residues by sulforaphane. *Chem. Res. Toxicol.* **2011**, 24 (4), 515–521.

- (30) Sthijns, M. M. J. P. E.; Weseler, A. R.; Bast, A.; Haenen, G. R. M. M. Time in Redox Adaptation Processes: From Evolution to Hormesis. *Int. J. Mol. Sci.* **2016**, *17* (10), 1649.
- (31) Jazwa, A.; Rojo, A. I.; Innamorato, N. G.; Hesse, M.; Fernández-Ruiz, J.; Cuadrado, A. Pharmacological targeting of the transcription factor Nrf2 at the basal ganglia provides disease modifying therapy for experimental parkinsonism. *Antioxid. Redox Signaling* **2011**, *14* (12), 2347–2360.
- (32) Srivastava, S.; Alfieri, A.; Siow, R. C. M.; Mann, G. E.; Fraser, P. A. Temporal and spatial distribution of Nrf2 in rat brain following stroke: quantification of nuclear to cytoplasmic Nrf2 content using a novel immunohistochemical technique. *J. Physiol.* **2013**, *591* (14), 3525–3538
- (33) Jang, M.; Cho, I.-H. Sulforaphane Ameliorates 3-Nitropropionic Acid-Induced Striatal Toxicity by Activating the Keap1-Nrf2-ARE Pathway and Inhibiting the MAPKs and NF-κB Pathways. *Mol. Neurobiol.* **2016**, *53* (4), 2619–2635.
- (34) Yao, W.; Zhang, J.; Ishima, T.; Dong, C.; Yang, C.; Ren, Q.; Ma, M.; Han, M.; Wu, J.; Suganuma, H.; et al. Role of Keap1-Nrf2 signaling in depression and dietary intake of glucoraphanin confers stress resilience in mice. *Sci. Rep.* **2016**, *6* (1), 30659.
- (35) Bricker, G. V.; Riedl, K. M.; Ralston, R. A.; Tober, K. L.; Oberyszyn, T. M.; Schwartz, S. J. Isothiocyanate metabolism, distribution, and interconversion in mice following consumption of thermally processed broccoli sprouts or purified sulforaphane. *Mol. Nutr. Food Res.* **2014**, *58* (10), 1991–2000.
- (36) Kassahun, K.; Davis, M.; Hu, P.; Martin, B.; Baillie, T. Biotransformation of the naturally occurring isothiocyanate sulforaphane in the rat: identification of phase I metabolites and glutathione conjugates. *Chem. Res. Toxicol.* **1997**, *10* (11), 1228–1233.
- (37) Clarke, J. D.; Hsu, A.; Riedl, K.; Bella, D.; Schwartz, S. J.; Stevens, J. F.; Ho, E. Bioavailability and inter-conversion of sulforaphane and erucin in human subjects consuming broccoli sprouts or broccoli supplement in a cross-over study design. *Pharmacol. Res.* **2011**, *64* (5), 456–463.
- (38) Munday, R.; Munday, C. M. Induction of phase II detoxification enzymes in rats by plant-derived isothiocyanates: comparison of allyl isothiocyanate with sulforaphane and related compounds. *J. Agric. Food Chem.* **2004**, *52* (7), 1867–1871.
- (39) Clarke, J. D.; Hsu, A.; Williams, D. E.; Dashwood, R. H.; Stevens, J. F.; Yamamoto, M.; Ho, E. Metabolism and tissue distribution of sulforaphane in Nrf2 knockout and wild-type mice. *Pharm. Res.* **2011**, 28 (12), 3171–3179.
- (40) Abbaoui, B.; Riedl, K. M.; Ralston, R. A.; Thomas-Ahner, J. M.; Schwartz, S. J.; Clinton, S. K.; Mortazavi, A. Inhibition of bladder cancer by broccoli isothiocyanates sulforaphane and erucin: characterization, metabolism, and interconversion. *Mol. Nutr. Food Res.* **2012**, 56 (11), 1675–1687.
- (41) Gasper, A. V.; Al-Janobi, A.; Smith, J. A.; Bacon, J. R.; Fortun, P.; Atherton, C.; Taylor, M. A.; Hawkey, C. J.; Barrett, D. A.; Mithen, R. F. Glutathione S-transferase M1 polymorphism and metabolism of sulforaphane from standard and high-glucosinolate broccoli. *Am. J. Clin. Nutr.* **2005**, 82 (6), 1283–1291.